Rapid Communications

Equilibrium field theory of magnetic monopoles in degenerate square spin ice: Correlations, entropic interactions, and charge screening regimes

Cristiano Nisoli

Theoretical Division, Los Alamos National Laboratory, Los Alamos, New Mexico 87545, USA

(Received 13 August 2020; revised 23 October 2020; accepted 18 November 2020; published 1 December 2020)

We describe degenerate square spin as an ensemble of magnetic monopoles coupled via an emergent entropic field that subsumes the effect of the underlying spin vacuum. We compute their effective free energy, entropic interaction, correlations, screening, and structure factor, and find that they coincide with the experimental ones. Unlike in pyrochlore ices, a dimensional mismatch between real and entropic interactions leads to weak singularities at the pinch points and algebraic correlations at long distances. This algebraic screening can be, however, camouflaged by a pseudoscreening regime.

DOI: 10.1103/PhysRevB.102.220401

Introduction. Magnetic monopoles [1,2] provide an emergent description of the low-energy physics of rare-earth spin ices [3–5] and have raised considerable interest, in particular, in regard to "magnetricity" [6–9]. Spin ices can be modeled [4,10,11] as systems of Ising spins on a pyrochlore lattice, impinging on tetrahedra such that their low-energy state obeys the Bernal-Fowler ice rule [12–14]: two spins point in, two out of each tetrahedron, realizing a degenerate manifold of constrained disorder [15,16] and residual entropy [3,14]. Then, violations of the ice rule can be interpreted as sinks or sources of the magnetization, i.e., charges, and the low-energy physics of spin ice can be described in terms of mobile deconfined *magnetic monopoles*, interacting via a Coulomb law in a disordered spin vacuum. Spin ice is, thus, a prominent platform in which monopole physics can be investigated.

Although experimental probes of monopoles in crystal-grown spin ices are necessarily indirect and at low temperatures, magnetic monopoles can now be characterized directly in real time, real space [17–20] at the desired temperature, and fields in *artificial spin ices* [21–25]. These two-dimensional (2D) arrays of magnetic, frustrated nanoislands are fabricated in a variety of geometries, often for exotic behaviors not found in natural magnets [26–33].

Here we study the monopoles of degenerate artificial square ice [34,35], recently realized in nanopatterned magnets [20,36,37] and in a quantum annealer [38]. Square ice provides a direct 2D analog of three-dimensional (3D) pyrochlore spin ice where monopole excitations can be directly characterized. Heuristic field theories of rare-earth pyrochlores [10,11,15,16] have dealt only with the ice manifold via a coarse-grained solenoidal field that describes the spin texture. We propose instead a framework where magnetic monopoles are the constitutive degrees of freedom, whereas the underlying spin ensemble is subsumed into entropic forces among these topological defects.

We show that, in the absence of physical interaction [38], monopoles interact *entropically* via a 2D-Coulomb logarithmic law, leading to $(2+1)$ electromagnetism, Bessel correlations of finite screening length for $T > 0$, and, thus, a conductive phase [39,40] where monopoles are unbound. The correlation length diverges at least exponentially as $T \downarrow 0$, signaling the criticality of the ice manifold. Then, inclusion of the monopole-monopole 3D-Coulomb interaction leads, unlike in 3D spin ice, to algebraic correlations and weak singularities in the structure factor at $T \neq 0$. Its interplay with the entropic interaction drives screening regimes of *effectively* bound and unbound monopoles.

(1) *Field theory.* Square ice is a set of N_e classical binary spins $\vec{S}_e$ aligned on the edges e of a square lattice of unit vectors $\hat{e}_1, \hat{e}_2$ of $N_v = N_e/2$ vertices labeled by v. The 16 spin configurations of a vertex are classified by four topologies [22,36] as t-I,..., t-IV (Fig. 1). Of each vertex, the charge $Q_v = 2n - 4$ is equal to the number n of spins pointing in minus the $4 - n$ pointing out. Then, $Q = 0$ for ice-rule obeying vertices (t-I and t-II). The following:

$$\mathcal{H}[Q] = \frac{\epsilon}{2}\sum_v Q_v^2 + \frac{\mu}{2}\sum_{v\neq v'} Q_v V_{vv'} Q_{v'} \tag{1}$$

is a suitable Hamiltonian for a variety of degenerate square ice realizations: ϵ is the cost of monopoles and $V_{vv'} = 1/2\pi|v - v'|$ is their 3D-Coulomb interaction; we take the lattice constant $a = 1$, and, thus, μ is an energy. When $\mu/\epsilon < 2\pi/M_\Box \simeq 3.9$ (where $M_\Box \simeq 1.6155$ is our Madelung constant [41]) the ground state is a disordered tessellation of the six ice-rule vertices (Fig. 1) of known Pauling entropy [42,43]. Above that threshold, the ground state becomes unstable toward the formation of a monopole ionic crystal.

In magnetic realizations [20,36,37], Eq. (1) corresponds to the dumbbell model of Ref. [2] (then ϵ is the coupling of the dumbbell charges in the vertex), the 3D-Coulomb interaction comes from the usual truncated multipole expansion, and, therefore, $\mu = \mu_0 p^2/l_d^2$, with p as the magnetic moment and $l_d < a$ as the dumbbell length. Then, $\mu/\epsilon \simeq 1 - l_d/a < 1$. Equation (1) does not describe the standard nondegenerate square ice [19,22,44–47] in which monopoles are confined by

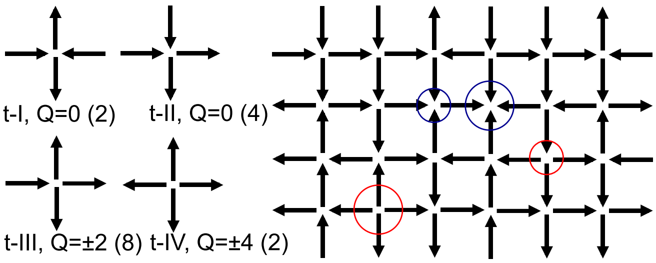

FIG. 1. Left: the four vertex configurations, ice-rule ones at the top ($Q = 0$) and the monopole at the bottom (multiplicities in parentheses). Right: portion of spin ice with monopoles of different charges circled.

the tension of magnetic Faraday lines [48–53]. Finally, even in realizations where ice-rule vertices are degenerate [34–38], the long-ranged dipolar interaction favors antiferromagnetic ordering [36] at $T \ll \epsilon$, an effect that we consider elsewhere.

The partition function is

$$Z[H] = \sum_S \exp\left(-\beta\mathcal{H} + \beta\sum_e \vec{S}_e \cdot \vec{H}_e\right), \tag{2}$$

($\beta = 1/T$) such that $\langle\vec{S}_{e_1}\cdots\vec{S}_{e_n}\rangle = \partial_{\beta\vec{H}_{e_1}\cdots\beta\vec{H}_{e_n}} \ln Z$. To sum over the spins, we insert the tautology [54] $1 = \prod_v \int dq_v d\phi_v \exp[i\phi_v(q_v - Q_v)]/(2\pi)^{N_v}$ obtaining

$$Z[H] = \int [dq] e^{-\beta\mathcal{H}[q]}\tilde{\Omega}[q], \tag{3}$$

where $[dq] = \prod_v dq_v/(2\pi)^{N_v}$ and the density of states,

$$\tilde{\Omega}[q] = \int [d\phi]\Omega[\phi] \exp\left(i\sum_v q_v\phi_v\right) \tag{4}$$

is the Fourier transform of the partition function for ϕ,

$$\Omega[\phi] = 2^{N_e}\prod_{\langle vv'\rangle}\cosh(-i\nabla_{vv'}\phi + \beta H_{vv'}) \tag{5}$$

(edges $\langle vv'\rangle$ are counted once, $\nabla_{vv'}\phi := \phi_{v'} - \phi_v$, $H_{vv'} := \vec{H}_e \cdot \hat{vv'}$). By construction, $\langle Q_{v_1}\cdots Q_{v_n}\rangle = \langle q_{v_1}\cdots q_{v_n}\rangle$.

We have obtained a theory of continuous charges constrained by an "entropy" $S[q] = \ln\tilde{\Omega}[q]$ conveying the effect of the spin ensemble. Equivalently, monopoles are coupled to an *entropic* field [55] $V_e = iT\phi$, of "free energy,"

$$\mathcal{F}[\phi] = -T\ \ln\Omega[\phi]. \tag{6}$$

From Eqs. (3)–(5) we have

$$\langle S_{vv'}\rangle = \langle\tanh(\beta H_{vv'} - i\nabla_{vv'}\phi)\rangle, \tag{7}$$

implying that whereas $V_e = iT\phi$ correlates charges, $B_e = iT\nabla\phi$ correlates spins that would be trivially paramagnetic in its absence. Note that $\overline{V}_{ev} := \langle V_{e,v}\rangle = iT\langle\phi_v\rangle$ is *real* [56]. In fact, the standard Gaussian gymnastic in the Supplemental Material [57] shows

$$\begin{aligned}\overline{V}_{e,v} &= \epsilon\overline{q}_v + \frac{\mu}{2\pi}\sum_{v'\neq v}\frac{\overline{q}_{v'}}{|v - v'|},\\ \overline{q} &= \sum_{\alpha=x,y}\partial^\alpha\overline{\tanh(\beta\,\partial_\alpha V_e - \beta H_\alpha)},\end{aligned} \tag{8}$$

with the second equation following from the definition of Q and from Eq. (7) in the continuum limit.

(2) *Approximations.* Equations (8) allow to compute the charge under boundary conditions in various approximations. For $\mu = 0$ their linearization returns screened-Poisson equations for q, V_e, of screening length,

$$\xi_0 = \sqrt{\epsilon/T}. \tag{9}$$

(A similar screening length had been found in different geometries via other methods [10,58], and, as we show elsewhere, holds for a general graph [59]). This approximation corresponds to a high-T limit. From Eqs. (3) and (4), by integrating over q_v one obtains $\langle\phi^2\rangle \simeq \epsilon/T$: as T increases the system loses correlation, and the entropic field decreases.

We can, therefore, legitimately expand $\mathcal{F}[\phi]$ in small ϕ. Then, Fourier transforming on the Brillouin zone (BZ) [60], we obtain the approximate partition function,

$$Z_{\text{eff}} = \int [dq\,d\phi]\exp\left(-\int_{\text{BZ}}\beta\mathcal{F}_{\text{eff}}[q,\phi](k)\frac{d^2k}{(2\pi)^2}\right), \tag{10}$$

of the free-energy functional at second order,

$$\begin{aligned}\mathcal{F}_{\text{eff}}[q,\phi] = \frac{\epsilon + \mu\tilde{V}}{2}|\tilde{q}|^2 + \frac{T}{2}\gamma^2|\tilde{\phi}|^2 - iT\tilde{q}^*\tilde{\phi}\\ -\tilde{\phi}^*\vec{\gamma}\cdot\vec{\tilde{H}} - \frac{\beta}{2}|\vec{\tilde{H}}|^2,\end{aligned} \tag{11}$$

where $\gamma_\alpha(\vec{k}) := 2\,\sin(k_\alpha/2)$ and $\tilde{V}(\vec{k})$ is the Fourier transform of V on the lattice. Integrating Z_{eff} over $\tilde{\phi}$ returns the *effective free energy for monopoles at quadratic order*,

$$\mathcal{F}_{\text{eff}}[q] = \frac{1}{2}\left(\epsilon + \mu\tilde{V} + \frac{T}{\gamma^2}\right)|\tilde{q}|^2. \tag{12}$$

The last term implies an entropic interaction among charges that at long distances ($\gamma^2 \simeq k^2$) is

$$V_e(\vec{r}_1 - \vec{r}_2) \simeq -T\frac{q_1q_2}{2\pi}\ln\|\vec{r}_1 - \vec{r}_2\|, \tag{13}$$

i.e., 2D Coulomb. Instead, in 3D, from Eq. (12) the entropic interaction would be 3D Coulomb, or $\sim 1/r$, thus, merely altering the coupling constant $\mu \to \mu + T$ of the real interaction as indeed found numerically [61,62]. The origin of the entropic interaction is the following: a charge assignation changes the degeneracy of the spin configurations compatible with it and, thus, the entropy. That the change in entropy can be written as the sum of pairwise logarithmic interactions is not obvious.

Equation (12) implies the charge correlations in k space,

$$\langle|\tilde{q}(\vec{k})|^2\rangle = \gamma(\vec{k})^2\tilde{\chi}_\parallel(\vec{k}), \tag{14}$$

with $\tilde{\chi}_\parallel(\vec{k})$ given by

$$\tilde{\chi}_\parallel(\vec{k})^{-1} = 1 + \xi_0{}^2\gamma(\vec{k})^2\left[1 + \frac{\mu}{\epsilon}\tilde{V}(k)\right]. \tag{15}$$

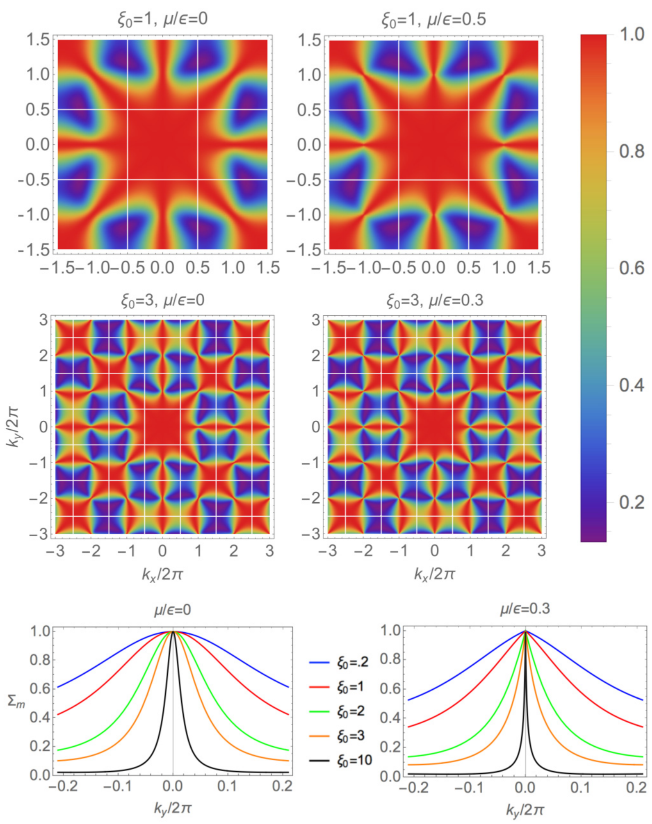

FIG. 2. Plots of structure factor Σ_m obtained from Eq. (17) for $\xi_0 = 0, 3,\ \mu/\epsilon = 0, 0.3, 0.5$ (k_x, k_y in units of $1/a$); $\mu > 0$ leads to sharper pinch points even at high T. Bottom row: Structure factor cuts on the line $k_x = 2\pi$ demonstrate discontinuity in the first derivative of the intensity when $\mu > 0$.

Note that $\langle|\tilde{q}(\vec{k})|^2\rangle$ peaks on the K points of the BZ. These peaks diverge when $\mu \uparrow (2\pi/M_\Box)(\epsilon + T/8)$, signaling the aforementioned instability toward an ionic crystal of ± 4 monopoles [63]. Note also that $\langle q^2\rangle = \int_{\mathrm{BZ}}\langle|\tilde{q}(\vec{k})|^2\rangle d^2k/(2\pi)^2 \uparrow 4$ as $T \uparrow \infty$, which is correct, as it can be verified by considering only vertex multiplicities $(2^2/2 + 4^2/8 = 4)$.

By performing the integral in Eq. (10) we obtain

$$\ln Z_{\mathrm{eff}} = \tfrac{1}{2}(\beta\vec{\tilde{H}}^*)\cdot(\hat{\gamma}\hat{\gamma}\tilde{\chi}_\parallel + {}^\perp\hat{\gamma}{}^\perp\hat{\gamma})\cdot(\beta\vec{\tilde{H}}) \tag{16}$$

($\hat{\gamma} := \vec{\gamma}/\gamma,\ {}^\perp\hat{\gamma} := \hat{e}_3 \wedge \hat{\gamma}$), showing that $\tilde{\chi}_\parallel(\vec{k})$ is the *longitudinal susceptibility* (multiplied by T). Thus,

$$\langle\tilde{S}^*_\alpha(\vec{k})\tilde{S}_{\alpha'}(\vec{k})\rangle = \hat{\gamma}_\alpha\hat{\gamma}_{\alpha'}\tilde{\chi}_\parallel + {}^\perp\hat{\gamma}_\alpha{}^\perp\hat{\gamma}_{\alpha'} \tag{17}$$

are the spin correlations, whose structure factor $\Sigma_m(\vec{k}) = {}^\perp\vec{k}\cdot\langle\vec{\tilde{S}}(\vec{k})\vec{\tilde{S}}(\vec{k})\rangle\cdot{}^\perp\vec{k}$ we plot in Fig. 2. In the limit $T \downarrow 0$ and, thus, $\xi_0 \uparrow \infty$, correlations in Eq. (17) become purely transversal. When $T > 0,\ \mu = 0$, pinch points are smoothened by a Lorentzian of width ξ_0. Instead, for $\mu \neq 0$ the profile is sharper with weak singularities controlled by the Bjerrum length $2l_B := \mu/T$,

$$\Sigma_m(2\pi, k_y) \simeq 1 - 2l_b|k_y| \quad \text{at } k_y \simeq 0, \tag{18}$$

due to the aforementioned dimensional mismatch.

To gain insight on how to proceed at low T [64], one could perturbatively expand $\mathcal{F}[\phi]$. Instead, we make the reasonable ansatz that the effective theory has the same functional form as $\mathcal{F}_{\mathrm{eff}}$ in Eq. (12) but with constants "dressed" by the interactions among fluctuations at low T. Note that $\xi_0 \uparrow \infty$ as $T \downarrow 0$ and Eq. (14) implies

$$\xi_0 \simeq 1/\sqrt{\langle q^2\rangle} \quad \text{for } T \downarrow 0, \tag{19}$$

and, therefore, ϵ is dressed as $\epsilon \to \epsilon(T) \sim T/\langle q^2\rangle$.

Then, if we approximate $\langle q^2\rangle$ by assuming uncorrelated vertices, we obtain $\xi_0 \simeq \exp(\epsilon/T)$. This exponential divergence of the correlation length (consistent with experimental findings [65]) points to the topological nature of the critical ice manifold at $T = 0$. Note that ξ_0 in Eq. (19) is exactly the Debye-Hückel [66] length for a Coulomb potential of coupling constant proportional to T as is the case of our entropic potential. In the Supplemental Material [57], a Debye-Hückel [61,67] approach inclusive of the entropic field [55] leads to the very same Eq. (14) *yet* with ξ_0 given by Eq. (19), corroborating our ansatz.

When $\mu = 0$, Eq. (12) reduces to a 2D-Coulomb gas with purely entropic interactions. From Eqs. (14) and (15) the charge correlations at long distances are

$$\langle q_{\vec{r}_1}q_{\vec{r}_2}\rangle \simeq -\frac{1}{2\pi\xi_0^4}K_0(\|\vec{r}_1 - \vec{r}_2\|/\xi_0), \tag{20}$$

as recently experimentally verified [38], showing that ξ_0 is indeed the correlation length. ξ_0 is also the screening length: A charge Q_{pin} pinned in v_0 elicits a charge distribution,

$$\overline{q}_v = Q_{\mathrm{pin}}\langle q_v q_{v_0}\rangle/\langle q^2\rangle. \tag{21}$$

A finite screening length implies that the system is conductive. There is no BKT transition [39,40] to an insulating phase at finite T (i.e., algebraic correlations and bound charges) because the interaction among charges is purely entropic, has coupling constant proportional to T, and, thus, no interplay between entropy and energy can drive a transition. The lack of such a transition can be shown, in general, from the model, regardless of our formalism [68]. Yet, when $\mu > 0$ the system is always insulating as we show now.

(3) *Monopole interactions and algebraic correlations.* Consider now $\mu > 0$. At small k, $\tilde{V}(k) \sim 1/k$ and Eq. (21) reads

$$\overline{\tilde{q}}(k) \simeq \frac{k^2}{1 + 2l_Bk + \xi_0^2k^2}\frac{Q_{\mathrm{pin}}}{\langle q^2\rangle}, \tag{22}$$

which is not analytical at $\vec{k} = 0$, leading to the aforementioned weak singularities at the pinch points. In 3D it would be analytical because $\tilde{V}(k) \sim 1/k^2$, the poles of $\overline{\tilde{q}}(k)$ would be purely imaginary [$k_\pm = \pm i/\xi_{3\mathrm{D}}$ with $\xi_{3\mathrm{D}}^{-2} = \xi_0^{-2}(1 + \mu/T)$], and, thus, $\xi_{3\mathrm{D}}$ would be a screening length. But in 2D the poles are $k_\pm = -\bar{k} \pm i/\xi_\mu$ with

$$\frac{\xi_\mu^2}{\xi_0^2} = \frac{\xi_0^2}{\xi_0^2 - l_B^2} = \frac{T}{T - T_\times}, \tag{23}$$

and they always have a real part $\bar{k} = l_B/\xi_0^2 = \mu/2\epsilon$.

Above the crossover temperature $T_\times = \mu^2/4\epsilon$, $\xi_0 > l_B$, ξ_μ is real, and poles have imaginary parts i/ξ_μ. Thus, one could heuristically consider ξ_μ a screening length, and say that above $T_\times$ monopoles are unbound, and the phase is conducive. Below $T_\times$, ξ_μ is imaginary, and one could say that there is no screening length, and monopoles are bound by the strength of the magnetic interaction ($\xi_0 < l_B$) in an insulating phase. However, things are more complicated than this naive picture would suggest.

In fact, mathematically speaking, there is *never* a finite screening length. To demonstrate it, consider a charge $Q_{\rm pin}$ pinned in the origin. From Eqs. (12) and (13), $\overline{\tilde{V}}_e(k) = T\overline{\tilde{q}}(k)/k^2$, and, thus, we obtain

$$\beta\overline{\tilde{V}}_e(k) = \frac{\xi_\mu}{2i\xi_0^2}\left(\frac{1}{k-k_+} - \frac{1}{k-k_-}\right)Q_{\rm pin}. \tag{24}$$

Using $2/c = \int_{-\infty}^{\infty}\exp(-|z|c)dz$ for $\mathrm{Re}(c) > 0$ on each fraction in Eq. (24) and Fourier transforming, we have

$$\beta\overline{V}_e(r) = \frac{l_B}{2\pi\langle q^2\rangle}\int_{-\infty}^{+\infty}\frac{\lambda(z)}{(r^2+z^2)^{3/2}}dz, \tag{25}$$

where $\lambda(z)$ can be interpreted as a linear charge density,

$$\lambda(z) = \frac{\xi_\mu}{2\xi_0^2 l_B}|z|\sin(|z|/\xi_\mu)e^{-\bar{k}|z|}Q_{\rm pin}, \tag{26}$$

for which $\int\lambda(z)dz = Q_{\rm pin}$. Therefore, the entropic potential can be represented as if generated by an *image* charge [69], spread along a line (of coordinate z) perpendicular to the 2D system, and of total charge $Q_{\rm pin}$.

Crucially, $\lambda(z)$ is exponentially confined by a length l. When $T > T_\times$, $l = 1/\bar{k}$. When $T < T_\times$, the sine in Eq. (26) becomes hyperbolic, and $l = 1/k_+$. For $r \gg l$ the charge is seen as pointlike, and the potential scales as

$$\overline{V}_e(r) \simeq \frac{l_B}{2\pi\langle q^2\rangle}\frac{Q_{\rm pin}}{r^3}, \tag{27}$$

and, by taking its Laplacian, $\overline{q}(r)$ scales as

$$\overline{q}(r) \simeq -\frac{9l_B}{2\pi\langle q^2\rangle}\frac{Q_{\rm pin}}{r^5}. \tag{28}$$

Remarkably, *long-distance screening—and, thus, spin correlations—are algebraic* at any T [Figs. 3(a) and 3(b)]. In 3D spin ice, instead, spin correlations are algebraic only at $T = 0$ even with monopole interaction. Algebraic screening from a 3D-Coulomb potential in the polarizability of quantum or classical 2D charge systems has been rediscovered multiple times [70–73]. In fact, it is not merely a 2D feature but can happen in any dimension for the same dimensional mismatch in the Coulomb interaction [74]. Importantly, unlike electrical charges, magnetic monopoles are emergent particles of a spin ensemble and interact entropically. The interplay between the correlation length at zero interaction (ξ_0) and the Bjerrum length (l_B) leads to a crossover at $T_\times$ between *effectively* conductive and insulating regimes.

To see that, consider

$$Q_{\rm alg}/Q_{\rm pin} \simeq -3l_B/\langle q^2\rangle l^3, \tag{29}$$

the fraction of the charge screened algebraically, obtained by integrating Eq. (28) for $x > l$. When it is very small, and l is large, the algebraic nature of the screening might not be detectable.

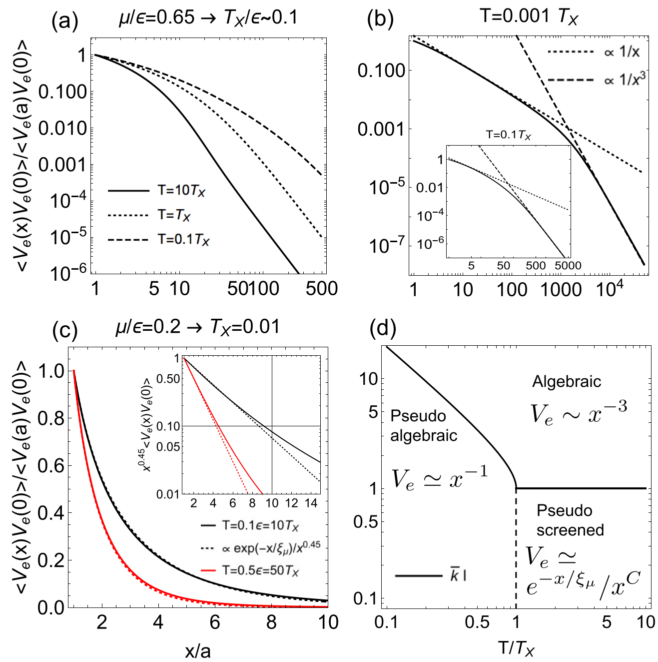

FIG. 3. Screening behavior at different T, μ's. (a) Log-log plots of the screening entropic potential $\overline{V}_e(x)$ (numerically integrated) of Eq. (25) for different temperatures at relatively strong monopole interaction $\mu = 0.65\epsilon$ leading to $l \simeq 3$ and $T_\times = 0.1\epsilon$ where our approximation should still apply. Note the algebraic $1/r^3$ decay. However, at high T the potential drops by 99% before becoming algebraic. (b) For $\mu = 0.65$ and $T/T_\times = 10^{-3}$, $\overline{V}_e(x)$ shows a pseudoalgebraic decay $\sim 1/r$ for most of its measurable tail (in the inset a higher-T case $T/T_\times = 0.1$). (c) At low monopole interaction ($\mu = 0.2\epsilon$) $T_\times/\epsilon = 0.01$ is very low, most of the charge is screened before the algebraic regime ($l = 10$). Effectively, the screening is exponential, and $V_e(x) \propto e^{-x/\xi_\mu}/x^{0.45}$ provides a good fit [in the inset, logarithmic plot of $x^{0.45}V_e(x)$]. (d) Plot of $\bar{k}l$ as a function of T and schematics of the screening at different distances.

When $T \gg T_\times$, $|Q_{\rm alg}/Q_{\rm pin}| \simeq 10^{-2}$ or less, and, thus, the algebraic screening might not be experimentally detectable. Moreover, as Fig. 3(c) shows, the screening within l is well fitted by an exponentially screened function. Thus, above $T_\times$ there is a "pseudoscreening length" $\xi_\mu > l_B$.

When $T \ll T_\times$ we can take $k_+ \sim 0$ and from Eq. (24) $\overline{\tilde{V}}_e(k) \sim 1/k$, and, thus, $\overline{V}_e(r) \sim 1/r$ for $r \ll l = 1/k_+$ [as confirmed by the numerical plot in Fig. 3(b)]. In this regime the insulating phase is easily detectable.

Considering l, $T_\times$, and $Q_{\rm alg}$, we can sketch heuristic regime diagrams, which are necessarily somehow arbitrary as they depend on practical specifications. Clearly, when l is smaller than, say, 2, the behavior is completely algebraic. When l is instead large, there might be pseudoscreening for $x < l$ if $T > T_\times$ and if most (we choose 99% in figure) of the charge is screened within a radius l (left side of the dashed line in Fig. 4). If $l \gg 2$ and $Q_{\rm alg}/Q_{\rm pin}$ is not small, an initial exponential screening for $r < l$ is followed by algebraic screening for $r \gg l$. Finally, note that ϵ gets dressed at low temperatures. At low μ/ϵ, the algebraic screening might be extremely hard to detect.

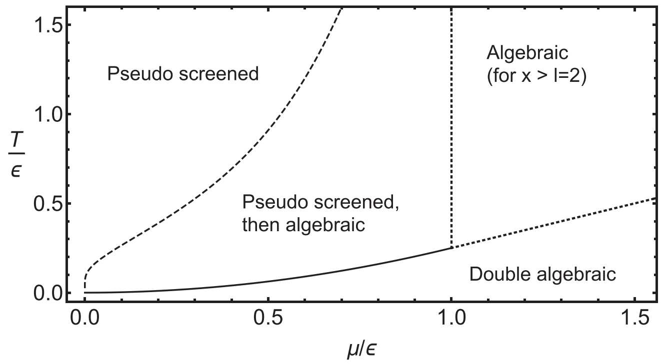

FIG. 4. Heuristic regime diagram. The solid line is $T_\times(\mu)$. The dashed line corresponds to 99% of the charge being screened within the radius l. On the right of the dotted line, $l \leqslant 2$, and there is, therefore, *algebraic* screening [$\langle q(r)q(0)\rangle \sim r^{-5}$]. On the left of the dashed line 99% of the charge is screened within l, and because $T > T_\times(\mu)$, the regime is *pseudoscreened*. In the *pseudoscreened, then the algebraic* regime, the behavior is effectively screened for $x < l$, but more than 1% of the charge is algebraically screened at $x > l$. In the *double algebraic* region $\langle q(r)q(0)\rangle \sim r^{-3}$ for $x \ll l$ and $\langle q(r)q(0)\rangle \sim r^{-5}$ for $x \gg l$. Note that in nanomagnetic realizations the dumbbell model imposes $\mu/\epsilon < 1$.

Conclusion. We have developed a field theory for monopoles in degenerate square ice. In the absence of a real monopole interaction the system is a 2D-Coulomb gas where monopoles interact entropically, are always screened and, thus, in an unbound, conductive phase. This case has been recently realized in quantum dots [38]. When the 3D-Coulomb interaction among monopoles is considered, reduced dimensionality prevents full screening, and a dimensional mismatch between Green's functions of the Laplace operator drive different effective screening regimes.

Our results, obtained via approximations on a simplified model, invite experimental tests which are, however, nontrivial: The algebraic behavior can be camouflaged by pseudoscreening if the monopole-monopole interaction is small. Algebraic correlations might be experimentally detectable in weak singularities near the pinch points from which the Bjerrum length can be extracted.

In the future, more precise expressions for various quantities can be computed by Feynman diagram expansion of $\mathcal{F}[\phi]$. The spirit of our approach can be applied also to 3D spin ice and to honeycomb/kagome spin ice [19,75] and can be extended to include topological currents beside charges, thus, underscoring the gauge-free duality of the square geometry.

Acknowledgments. We thank Beatrice Nisoli for proofreading. This work was carried out under the auspices of the U.S. DoE through the Los 405 Alamos National Laboratory, operated by Triad National 406 Security, LLC (Contract No. 892333218NCA000001).

[1] I. Ryzhkin, J. Exp. Theor. Phys. **101**, 481 (2005).
[2] C. Castelnovo, R. Moessner, and S. L. Sondhi, Nature (London) **451**, 42 (2008).
[3] A. P. Ramirez, A. Hayashi, R. J. Cava, R. Siddharthan, and B. S. Shastry, Nature (London) **399**, 333 (1999).
[4] B. C. den Hertog and M. J. P. Gingras, Phys. Rev. Lett. **84**, 3430 (2000).
[5] S. T. Bramwell and M. J. Gingras, Science **294**, 1495 (2001).
[6] D. J. P. Morris, D. Tennant, S. Grigera, B. Klemke, C. Castelnovo, R. Moessner, C. Czternasty, M. Meissner, K. Rule, J.-U. Hoffmann *et al.*, Science **326**, 411 (2009).
[7] S. R. Giblin, S. T. Bramwell, P. C. W. Holdsworth, D. Prabhakaran, and I. Terry, Nat. Phys. **7**, 252 (2011).
[8] S. J. Blundell, Phys. Rev. Lett. **108**, 147601 (2012).
[9] F. K. K. Kirschner, F. Flicker, A. Yacoby, N. Y. Yao, and S. J. Blundell, Phys. Rev. B **97**, 140402(R) (2018).
[10] C. L. Henley, Phys. Rev. B **71**, 014424 (2005).
[11] S. V. Isakov, K. Gregor, R. Moessner, and S. L. Sondhi, Phys. Rev. Lett. **93**, 167204 (2004).
[12] W. Giauque and J. Stout, J. Am. Chem. Soc. **58**, 1144 (1936).
[13] J. Bernal and R. Fowler, J. Chem. Phys. **1**, 515 (1933).
[14] L. Pauling, J. Am. Chem. Soc. **57**, 2680 (1935).
[15] C. L. Henley, Annu. Rev. Condens. Matter Phys. **1**, 179 (2010).
[16] C. Castelnovo, ChemPhysChem **11**, 557 (2010).
[17] S. Ladak, D. Read, W. Branford, and L. Cohen, New J. Phys. **13**, 063032 (2011).
[18] E. Mengotti, L. J. Heyderman, A. F. Rodríguez, F. Nolting, R. V. Hügli, and H.-B. Braun, Nat. Phys. **7**, 68 (2010).
[19] S. Zhang, I. Gilbert, C. Nisoli, G.-W. Chern, M. J. Erickson, L. O'Brien, C. Leighton, P. E. Lammert, V. H. Crespi, and P. Schiffer, Nature (London) **500**, 553 (2013).
[20] A. Farhan, M. Saccone, C. F. Petersen, S. Dhuey, R. V. Chopdekar, Y.-L. Huang, N. Kent, Z. Chen, M. J. Alava, T. Lippert *et al.*, Sci. Adv. **5**, eaav6380 (2019).
[21] M. Tanaka, E. Saitoh, H. Miyajima, T. Yamaoka, and Y. Iye, Phys. Rev. B **73**, 052411 (2006).
[22] R. F. Wang, C. Nisoli, R. S. Freitas, J. Li, W. McConville, B. J. Cooley, M. S. Lund, N. Samarth, C. Leighton, V. H. Crespi, and P. Schiffer, Nature (London) **439**, 303 (2006).
[23] C. Nisoli, R. Moessner, and P. Schiffer, Rev. Mod. Phys. **85**, 1473 (2013).
[24] L. Heyderman and R. Stamps, J. Phys.: Condens. Matter **25**, 363201 (2013).
[25] A. Ortiz-Ambriz, C. Nisoli, C. Reichhardt, C. J. O. Reichhardt, and P. Tierno, Rev. Mod. Phys. **91**, 041003 (2019).
[26] M. J. Morrison, T. R. Nelson, and C. Nisoli, New J. Phys. **15**, 045009 (2013).
[27] A. Farhan, C. F. Petersen, S. Dhuey, L. Anghinolfi, Q. H. Qin, M. Saccone, S. Velten, C. Wuth, S. Gliga, P. Mellado *et al.*, Nat. Commun. **8**, 1 (2017).
[28] V. Bhat, B. Farmer, N. Smith, E. Teipel, J. Woods, J. Sklenar, J. B. Ketterson, J. Hastings, and L. De Long, Physica C **503**, 170 (2014).
[29] D. Shi, Z. Budrikis, A. Stein, S. A. Morley, P. D. Olmsted, G. Burnell, and C. H. Marrows, Nat. Phys. **14**, 309 (2018).
[30] C. Nisoli, Frustration(s) and the Ice Rule: From Natural Materials to the Deliberate Design of Exotic Behaviors, in *Frustrated Materials and Ferroic Glasses*, edited by T. Lookman and X. Ren, Springer Series in Materials Science, Vol. 275 (Springer, Cham, 2018), pp. 57–99.
[31] S. H. Skjærvø, C. H. Marrows, R. L. Stamps, and L. J. Heyderman, Nat. Rev. Phys. **2**, 13 (2020).

[32] S. Gliga, G. Seniutinas, A. Weber, and C. David, Mater. Today **26**, 100 (2019).
[33] J. Sklenar, Y. Lao, A. Albrecht, J. D. Watts, C. Nisoli, G.-W. Chern, and P. Schiffer, Nat. Phys. **15**, 191 (2019).
[34] G. Möller and R. Moessner, Phys. Rev. Lett. **96**, 237202 (2006).
[35] V. Schanilec, Y. Perrin, S. L. Denmat, B. Canals, and N. Rougemaille, arXiv:1902.00452.
[36] Y. Perrin, B. Canals, and N. Rougemaille, Nature (London) **540**, 410 (2016).
[37] E. Östman, H. Stopfel, I.-A. Chioar, U. B. Arnalds, A. Stein, V. Kapaklis, and B. Hjörvarsson, Nat. Phys. **14**, 375 (2018).
[38] A. D. King, C. Nisoli, E. D. Dahl, G. Poulin-Lamarre, and A. Lopez-Bezanilla, arXiv:2007.10555.
[39] V. Berezinskii, Sov. Phys. JETP **32**, 493 (1971).
[40] J. M. Kosterlitz and D. J. Thouless, J. Phys. C **6**, 1181 (1973).
[41] D. Borwein, J. M. Borwein, and K. F. Taylor, J. Math. Phys. **26**, 2999 (1985).
[42] E. H. Lieb, Phys. Rev. **162**, 162 (1967).
[43] R. Baxter, *Exactly Solved Models in Statistical Mechanics* (Academic, New York, 1982).
[44] C. Nisoli, J. Li, X. Ke, D. Garand, P. Schiffer, and V. H. Crespi, Phys. Rev. Lett. **105**, 047205 (2010).
[45] J. P. Morgan, A. Stein, S. Langridge, and C. H. Marrows, Nat. Phys. **7**, 75 (2010).
[46] J. Porro, A. Bedoya-Pinto, A. Berger, and P. Vavassori, New J. Phys. **15**, 055012 (2013).
[47] O. Sendetskyi, V. Scagnoli, N. Leo, L. Anghinolfi, A. Alberca, J. Lüning, U. Staub, P. M. Derlet, and L. J. Heyderman, Phys. Rev. B **99**, 214430 (2019).
[48] L. Mól, R. Silva, R. Silva, A. Pereira, W. Moura-Melo, and B. Costa, J. Appl. Phys. **106**, 063913 (2009).
[49] R. Silva, F. Nascimento, L. Mól, W. Moura-Melo, and A. Pereira, New J. Phys. **14**, 015008 (2012).
[50] R. C. Silva, R. J. C. Lopes, L. A. S. Mól, W. A. Moura-Melo, G. M. Wysin, and A. R. Pereira, Phys. Rev. B **87**, 014414 (2013).
[51] D. Levis, L. F. Cugliandolo, L. Foini, and M. Tarzia, Phys. Rev. Lett. **110**, 207206 (2013).
[52] C. Nisoli, arXiv:2004.02107.
[53] L. Foini, D. Levis, M. Tarzia, and L. F. Cugliandolo, J. Stat. Mech.: Theory Exp. (2013) P02026.
[54] J. Hubbard, Phys. Rev. Lett. **3**, 77 (1959).
[55] C. Nisoli, New J. Phys. **16**, 113049 (2014).
[56] We denote one-point functions with an overline.
[57] See Supplemental Material at http://link.aps.org/supplemental/10.1103/PhysRevB.102.220401 for further derivations.
[58] D. A. Garanin and B. Canals, Phys. Rev. B **59**, 443 (1999).
[59] C. Nisoli, AIP Adv. **10**, 115102 (2020).
[60] $g(\vec{r}) = \int_{\mathrm{BZ}} \tilde{g}(\vec{k}) e^{-i\vec{k}\cdot\vec{r}} d^2k/(2\pi)^2$ with g a general function, $\vec{r} = v, e$ vertices or edges.
[61] C. Castelnovo, R. Moessner, and S. L. Sondhi, Phys. Rev. B **84**, 144435 (2011).
[62] G.-W. Chern, C. Reichhardt, and C. Nisoli, Appl. Phys. Lett. **104**, 013101 (2014).
[63] Such large μ values are unattainable in a dumbbell model, thus, they are hard to realize in magnetic spin ice.
[64] Low but "not too low." At really low T ordering can take place as discussed but also glassy kinetics and nonequilibration.
[65] T. Fennell, P. Deen, A. Wildes, K. Schmalzl, D. Prabhakaran, A. Boothroyd, R. Aldus, D. McMorrow, and S. Bramwell, Science **326**, 415 (2009).
[66] Y. Levin, Rep. Prog. Phys. **65**, 1577 (2002).
[67] V. Kaiser, J. Bloxsom, L. Bovo, S. T. Bramwell, P. C. W. Holdsworth, and R. Moessner, Phys. Rev. B **98**, 144413 (2018).
[68] Nonetheless, it is possible to show that the state at $T = 0$ does belong to the critical portion of the KT transition, and indeed the correlation length is infinite.
[69] J. D. Jackson, *Classical Electrodynamics* (Wiley, Hoboken, NJ, 2007).
[70] T. Ando, A. B. Fowler, and F. Stern, Rev. Mod. Phys. **54**, 437 (1982).
[71] L. Keldysh, JETP Lett. **29**, 658 (1979).
[72] D. Jena and A. Konar, Phys. Rev. Lett. **98**, 136805 (2007).
[73] P. Cudazzo, I. V. Tokatly, and A. Rubio, Phys. Rev. B **84**, 085406 (2011).
[74] C. Nisoli (unpublished).
[75] Y. Qi, T. Brintlinger, and J. Cumings, Phys. Rev. B **77**, 094418 (2008).